Cavity-Creating Mutation at the Dimer Interface of *Plasmodium falciparum* Triosephosphate Isomerase: Restoration of Stability by Disulfide Cross-Linking of Subunits†

B. Gopal,‡ Soumya S. Ray,‡ R. S. Gokhale,‡ H. Balaram,§ M. R. N. Murthy,‡ and P. Balaram*,‡,||

Molecular Biophysics Unit, Indian Institute of Science, Bangalore 560 012, India, and Molecular Biology and Genetics Unit and Chemical Biology Unit, Jawaharlal Nehru Center for Advanced Scientific Research, Jakkur, Bangalore 560 064, India

Received July 2, 1998; Revised Manuscript Received September 29, 1998

ABSTRACT: Disulfide engineering across subunit interfaces provides a means of inhibiting dissociation during unfolding of multimeric enzymes. Two symmetry-related intersubunit disulfide bridges were introduced across the interface of the dimeric enzyme triosephosphate isomerase from *Plasmodium falciparum*. This was achieved by mutating a tyrosine residue at position 74 at the subunit interface to a cysteine, thereby enabling it to form a covalent cross-link with a pre-existing cysteine at position 13 of the other subunit. The wild-type enzyme (TIMWT) and the oxidized (Y74Cox) and reduced (Y74Cred) forms of the mutant have similar enzymatic activity, absorption, and fluorescence spectra. All three proteins have similar far-UV CD spectra. The Y74Cred shows a distinct loss of near-UV CD. Thermal precipitation studies demonstrate that TIMWT and Y74Cox have very similar T_m values ($T_m \sim 60$ °C) whereas Y74Cred is surprisingly labile ($T_m \sim 38$ °C). The Y74C mutant results in the creation of a large cavity (∼100 Å^3) at the dimer interface. The crystal structure for the oxidized form of Y74C mutant, crystallized in the presence of low concentrations of dithiothreitol, reveals an asymmetric dimer containing a disulfide bridge at one site and a reduced dithiol cysteine at the other. The crystal structure of the mutant offers insights into the destabilization effects of the interfacial cavities and the role of disulfide tethering in restoring protein stability.

Small monomeric proteins containing multiple disulfide bridges are generally resistant to both thermal and chaotrope-induced unfolding. Two well-studied proteins, hen egg white lysozyme and ribonuclease, which have four disulfide cross-links, are stable to temperatures greater than 70 °C (*1*−*4*). There are relatively few examples of native multimeric proteins with intersubunit disulfide bonds (*5*). Attempts to enhance the thermostability of proteins by redesigning hydrophobic cores, by introducing ionic interactions, or by stabilizing helices have generally resulted in marginal increases in protein stability (*6*). In this context, the engineering of disulfide bridges, the only *natural* mode of covalently tethering structural units, might be a viable approach to protein stabilization.

Intersubunit disulfide engineering with λ-repressor (*7*), λ-cro (*8*), glutathione reductase (*9*), and xylanase (*10*) has resulted in mixed success in enhancing stability. In all of these proteins, one disulfide cross-link was introduced across the subunit interface. Introduction of symmetrical disulfide bridges across the dimeric interface of thymidylate synthase has been shown to dramatically increase the thermal stability of the protein (*11*). Further, covalent cross-linking also abolished the appearance of chaotrope-induced aggregates at intermediate concentrations of the denaturants urea and guanidinium chloride (GdmCl)[1] (*12*, *13*). Disulfide cross-linking of protein subunits has also been used to analyze the entropic cost of protein association (*14*). To explore the effects of disulfide cross-links on dimeric proteins in general, we have investigated the reduced and oxidized forms of the Y74C mutant of *Plasmodium falciparum* triosephosphate isomerase (PfTIM). Here we describe the crystal structure and the stability of an intersubunit disulfide-bonded mutant of TIM. TIM is a prototype of an eight-stranded α/β-barrel topology, in which the protein interface is primarily composed of loops (*15*) and serves as a good model system to study the folding of multimeric proteins. The Y74C mutant permits the formation of a symmetry-related disulfide bond between residues 13 and 74′ on adjacent subunits. The stability of the oxidized form of the mutant is similar to that of the wild type, whereas, surprisingly, the reduced form was remarkably unstable. The studies presented here suggest that formation of a cavity at the TIM dimer interface by replacement of Tyr 74 by Cys results in dramatic destabiliza-

† This work was supported by grants from the Council for Scientific and Industrial Research, Govt. of India to M.R.N.M. and P.B.

* Corresponding Author: P. Balaram, Molecular Biophysics Unit, Indian Institute of Science, Bangalore, India 560 012. E-mail: pb@mbu.iisc.ernet.in. Fax: +91-80-3348535, +91-80-3341683.

‡ Indian Institute of Science.

§ Molecular Biology and Genetics Unit, Jawaharlal Nehru Center for Advanced Scientific Research.

|| Chemical Biology Unit, Jawaharlal Nehru Center for Advanced Scientific Research.

[1] Abbreviations: GdmCl, guanidinium chloride; PfTIM, *Plasmodium falciparum* triosephosphate isomerase; TrisCl, Tris[hydroxymethyl]-amino methane; EDTA, ethylenediaminetetraacetic acid disodium salt; DTNB, 5,5′-dithiobis(2-nitrobenzoic acid); CD, circular dichroism; TIMWT, wild-type PfTIM; Y74Cox, oxidized form of the Y74C mutant of PfTIM; Y74Cred, reduced form of the Y74C mutant.

10.1021/bi981495w CCC: $18.00
Published on Web 12/15/1998

tion. Stability can then be restored by covalent tethering of the dimer interface by disulfide bonds.

MATERIALS AND METHODS

Purification of TIMWT. The PfTIM gene was cloned into pTrc 99A vector, called pARC1008 (*16*). The protein was overexpressed in the *Escherichia coli* strain AA200, which has a null mutation in the host TIM gene (*17*). The detailed purification procedure has been published (*18*). Mutagenesis was carried out using Kunkel's method (*19*), using a subclone of TIMWT in pBSK$^+$. The mutant was cloned back into pTRC99A. The cell lysate was subjected to ammonium sulfate precipitation. Y74C could be selectively precipitated at 95% saturated ammonium sulfate (63% w/v). Following this, the protein was further purified by ion exchange chromatography on a Pharmacia FPLC system. Yields up to 75 mg/L of *E. coli* culture were routinely obtained. The procedure for the purification of the mutant was similar to PfTIM. The oxidation of the mutant to Y74Cox was carried out by air oxidation using extensive dialysis in 20 mM TrisCl buffer (pH 8.0) for 24 h. Protein concentrations of less than 1 mg/mL were used for dialysis. Specific activities of the three proteins TIMWT, Y74Cox, and Y74Cred are 8965, 8426, and 8605 units/mg, respectively.

UV Absorbance, Fluorescence, and Circular Dichroism Measurements. UV measurements were carried out on a JASCO UV spectrophotometer using 4 μM protein, equilibrated in 100 mM TrisCl, pH 8.0, prior to measurements.

Fluorescence emission spectra were recorded on a Hitachi 650-60 spectrofluorimeter. Protein samples were excited at 280 nm, and the emission was recorded over a range of 300−400 nm. Excitation and emission band-pass were set at 5 nm. A protein concentration of 2 μM was used for fluorescence measurements.

Circular dichroism measurements were carried out on a JASCO J500A spectropolarimeter attached to a DP501N data processer. Ellipticity changes were monitored over the range 200−250 nm for far-UV CD using a path length of 1 mm. The near-UV band was followed using a 5 mm path length cuvette, at a protein concentration of 28 μM. Near-UV CD spectra were recorded over a range of 250−300 nm. Spectra were averaged over 2−4 scans at a scan speed of 10 nm/min.

Estimation of Cysteine Residues. Thiol estimation was carried out using Ellman's method (*20*) using DTNB. Protein (4 μM) was incubated with a 5-fold molar excess of DTNB in 100 mM TrisCl, pH 8.0, for $^1/_2$ h. Following this, the OD was measured at 412 nm. For measurement of thiols in the reduced protein, 100 μM protein was reduced with 1 mM DTT and then passed through a 10 mL Sephadex G10 desalting column. The desalting was carried out in 50 mM TrisCl, pH 6.0, to prevent reoxidation of cysteine residues to disulfide during the course of gel filtration. Following gel filtration, the protein concentration was adjusted to 4 μM in 100 mM TrisCl, pH 8.0, for thiol estimation.

Crystallization and X-ray Data Analysis. Crystals of the Y74C mutant of PfTIM were obtained using the hanging drop method. The reservoir solution contained 15% PEG 8000, 10 mM calcium chloride, and 0.05 mM each of DTT, EDTA, and sodium azide in 100 mM MES buffer, pH 6.5. Crystals were obtained in a 6 μL drop containing 3 μL of the reservoir solution and 3 μL of protein (20 mg/mL) placed on a presiliconized cover-slip equilibrated with the reservoir solution. The crystals grew over a period of five months to a size of 0.6 × 0.3 × 0.2 mm. It was essential to have 0.05 mM DTT and EDTA in the crystallization droplet. Crystallization setups without these additives were observed to result in a precipitate within 3 days and did not yield any crystals. The crystals belong to the monoclinic space group $P2_1$, with $a = 40.6$ Å, $b = 77.3$ Å, $c = 78.6$ Å, and $\beta = 100.7°$. The asymmetric unit of the crystal is compatible with one dimer (Matthews coefficient = 2.1265 Å^3/Da, assuming a molecular mass of 28 kDa/monomer). The X-ray diffraction data were collected at 23 ± 2 °C on a MAR image plate attached to a Rigaku RU-200 rotating anode X-ray generator. The structure was determined using the molecular replacement program AMoRe (*21*) using wild-type PfTIM coordinates (*18*) and refined using X-PLOR (*22*).

RESULTS

Design of Mutation. An interesting feature of PfTIM is the presence of a cysteine residue at position 13 which is a part of the dimer interface (*16*, *18*). This residue is conserved in *Trypanosomal* TIM (TryTIM) also. The engineering of a suitably positioned Cys residue on the complementary subunit would then permit disulfide bond formation with Cys13. An appropriate mutation site was identified using the disulfide modeling routine, MODIP, developed earlier in our laboratory (*23*). Briefly the program uses as input the Cα and Cβ coordinates from a protein crystal structure and identifies residue pairs where the Cα−Cα and Cβ−Cβ distances fall within the ranges expected for disulfide bonds in proteins ($r_{ij\alpha} \leq 6.5$ Å and $r_{ij\beta} \leq 4.5$ Å). Subsequently the program setreochemically fixes the two sulfur atoms at the chosen sites using standard geometries at disulfide linkages derived from high-resolution crystal structures of peptides. In principle, the modeling procedure can yield up to four unique positions for the two sulfur atoms. The modeled disulfide bridges are then evaluated for their stereochemical acceptability and assigned a letter grade A, B, or C depending upon the modeled stereochemical parameters. Using TryTIM (5TIM) coordinates, the MODIP routine identified residue 74 (Tyr in PfTIM and Phe in TryTIM) as a suitable site. The stereochemistry of the modeled disulfide was excellent (grade A in MODIP ranking). The crystal structure of PfTIM solved recently in our laboratory (*18*) after the initial disulfide modeling studies shows that the overall fold of TryTIM is maintained in PfTIM, thus validating the use of 5TIM coordinates for identifying the mutation site. However, in the case of the PfTIM coordinates determined at 2.2 Å resolution, the two modeled S−S bridges were asymmetric, with one having excellent stereochemistry while the other was appreciably constrained (grade C in the MODIP ranking, Table 1). This is of relevance in considering the crystal structure of the Y74C mutant discussed later. The Y74C mutant of PfTIM in its oxidized state is anticipated to possess two symmetrically placed intersubunit disulfide bridges (13−74′ and 74−13′). It may be noted that the distance $r_{ij\beta}$ of the Cβ atoms of residues 13−13′ is 21.35 Å and the corresponding $r_{ij\beta}$ for residues 74−74′ is 22.62 Å ruling out the possibility of disulfide bond formation between these thiol groups in the absence of major structural reorientation at the interface. It is also pertinent to note that oxidation of the

Table 1: Stereochemical Parameters for Modeled Disulfide Bridges in PfTIM using MODIP[a]

residues	r(S-S)	ChiSS	Chi1I	Chi1J	Chi2I	Chi2J	grade
PfTIM							
Cys A13-Tyr B 74[b]							
(i)	1.819	115.4	34.4	30.7	−174.7	17.3	A
(ii)	2.561	169.5	34.4	87.6	−145.3	−61.8	C
(iii)	2.572	−172.4	−35.5	30.7	143.2	59.8	C
(iv)	1.871	−118.6	−35.5	87.6	174.2	−17.8	A
Tyr A74-Cys B13[b]							
(i)	1.879	126.9	34.7	23.1	14.8	−174.9	C
(ii)	2.428	−171.0	34.7	−38.0	56.6	146.9	C
(iii)	2.437	173.7	84.0	23.1	−54.5	−144.8	C
(iv)	1.831	−123.9	84.0	−38.0	−13.9	175.8	C
Y74C							
Cys A13-Cys B74[c]							
(i)	2.408	58.7	63.0	−41.6	173.6	46.7	C
(ii)	4.049	173.8	63.0	97.1	−156.4	−82.4	C
(iii)	3.283	−92.9	−134.3	−41.6	−170.7	115.3	C
(iv)	2.171	44.2	−134.3	97.1	127.7	−105.4	C

[a] The PfTIM coordinates at 2.2 Å were used in the modeling. The description of the stereochemical parameters and acceptable ranges are given in Sowdhamini et al., 1989 (*21*). The two sets of modeled values correspond to the bridges 13−74′ and 74−13′. The lack of symmetry is evident. [b] Relevent Cα−Cα and Cβ−Cβ distances are as follows: CYS A 13, TYR B 74, Cα−Cα = 5.559, Cβ−Cβ = 4.396; TYR A 74, CYS B 13, Cα−Cα = 5.629, Cβ−Cβ = 4.475. [c] The backbone and Cβ coordinates determined for Y74C used in this study were used for modelling. The relevant Cα−Cα and Cβ−Cβ distances are as CYS A 13, CYS B 74, Cα−Cα = 4.564, Cβ−Cβ = 3.096; CYS A 74, CYS B 13, Cα−Cα = 4.268 Cβ−Cβ = 4.611. Sulfur cannot be fixed for the site Cys A74−Cys B13.

wild-type enzyme PfTIM which possess cysteine residues at positions 13 and 13′ does not yield any covalently cross-linked product as judged by SDS−PAGE. Figure 1 shows the location of the site of mutation. Site-directed mutagenesis was carried out using Kunkel's procedure (*19*). The Y74C mutant clone was identified using a restriction selection method and confirmed by DNA sequencing.

Characterization of the Mutant Protein. The mutant protein Y74C, obtained by the overexpression of the corresponding gene in *E. coli* strain AA200 (null for TIM), was isolated in the reduced form (Y74Cred). Oxidation to the disulfide dimer (Y74Cox) was achieved by air oxidation at pH 8.0. DTNB-mediated disulfide formation resulted in protein precipitation. The reason for such behavior has not been investigated, although we believe that any modification of the interface Cys13 residue is detrimental to protein stability. Similar behavior was also observed for the wild-type protein when carboxymethylation of thiols was carried out using iodoacetamide or iodoacetic acid (*18*). Thiol estimations were carried out on the reduced and oxidized forms of Y74C and compared with the values obtained for the wild-type enzyme (TIMwt) (Table 2). The Y74Cox shows 6 free cysteines as compared to Y74Cred which has 10 free cysteines, indicating the formation of two disulfide bridges. Figure 2 compares the electrophoretic mobility of the oxidized and the reduced forms of the protein. Lane 4 shows the dimeric protein migrating as a ∼54 kDa molecular mass band under nonreducing conditions. The reduced protein comigrates with PfTIM as shown in lanes 2 and 3, respectively. Specific activities of the three proteins TIMWT, Y74Cox, and Y74Cred are 8965, 8426, and 8605 units/mg, respectively. The mutation at the dimer interface did not result in a marked change in the specific activity of the protein at ambient temperature.

Comparison of the UV spectra for TIMWT, Y74Cox, and Y74Cred indicated a lower absorption for the mutant at 280 nm (Figure 3A). This is probably due to the loss of contribution of Tyr74 to the overall UV spectrum of the protein. PfTIM contains 7 Tyr and 2 Trp residues. Fluorescence spectra for the three proteins are shown in Figure 3B. Y74C has a lower quantum yield as compared to TIMWT. It is interesting to note that the reduced form of Y74C has a higher quantum yield as compared to the oxidized form. This is probably due to the quenching of Trp11 emission, which is adjacent to the disulfide bond. Enhancement of tryptophan fluorescence upon reduction of proximal disulfides is commonly observed in proteins and is exemplified by the case of thioredoxin (*24*). The far-UV CD spectra of TIMWT, Y74Cox, and Y74Cred are shown in Figure 4A. The spectra for both proteins are almost similar, with 2% lower ellipticity for the mutant protein at 222 nm. This indicates that there are no major changes in the overall secondary structure of the protein due to the mutation and subsequent oxidization to the disulfide form. Interestingly, the near-UV CD spectrum for Y74Cred showed a surpising loss of ellipticity (Figure 4B) as compared to Y74Cox and TIMWT. This may be due to the replacement of the tyrosine residue at position 74 and the attendant loss of optimal packing interactions at the site of mutation.

Specific Activity. Enzymatic activity of PfTIM was monitored using a coupled enzyme assay which requires the use of α-glycerophosphate dehydrogenase. Measurements of the activity at varying temperatures are therefore complicated by the simultaneous effects of heating on two enzymes. For assessing the stability, PfTIM was incubated separately at various temperatures for a fixed period of time (10 min), after which the activity was measured at ambient temperature (25 °C). It is observed that PfTIM has an "optimum incubation temperature" of approximately 40 °C, with complete abolition of activity beyond 60 °C. Y74Cox mutant protein also shows maximum activity after incubation at 40 °C, although the measured specific activity at 40 °C of Y74Cox under these conditions is only 50% of the PfTIM activity at the same temperature. It should be noted that the specific activities of Y74Cox and PfTIM are similar when the enzymes were incubated at 25 °C. The activity of Y74Cox is also completely abolished by 60 °C.

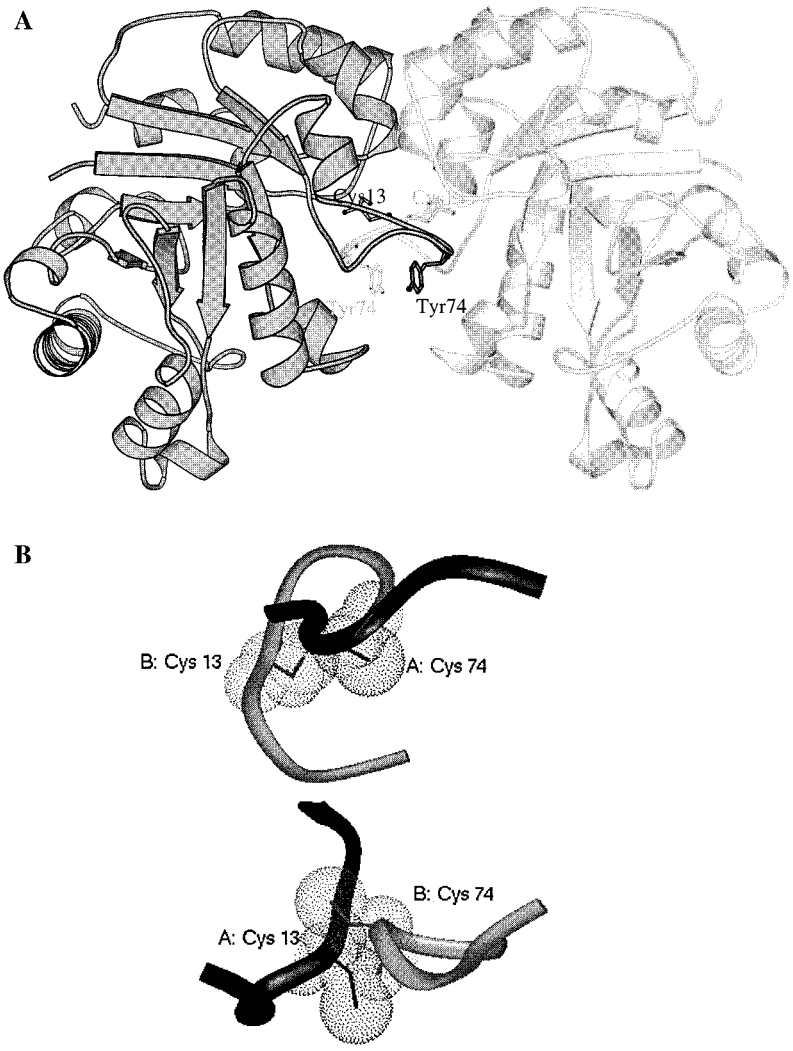

FIGURE 1: (A) Ribbon drawing of the molecule of PfTIM (Velanker et al., 1997) prepared using MOLSCRIPT (Kraulis, 1994). The site of mutation, residue 74 (Cys), is shown. Cys 13 is also indicated. The two monomers are drawn in different shades. (B) A close-up view of the dimer interface at the site of mutation in the two subunits.

Table 2: Thiol Estimation for TIMWT and the Oxidized/Reduced Forms of the Mutant Y74C[a]

protein sample	no. of thiols obtained per dimer	av no. of thiols per dimer	no. of thiols per dimer from protein sequences
TIMWT	8.1 8.6 8.5	8.4	8.0
Y74Cox	5.8 5.9 6.3	6.0	6.0
Y74Cred	10.2 9.5 9.7	9.8	10.0

[a] Thiol estimation was carried out using Ellman's reagent (*17*). The protein was incubated with 6 M GdmCl for one hour prior to thiol estimation. The molar extinction coefficient of DTNB is taken to be 13 600 cm^{-1} at 412 nm. The molar extinction coefficients of TIMWT, Y74Cox, and Y74Cred were calculated to be 41 640, 39 340, and 39 310 M^{-1} cm^{-1} at 280 nm, respectively, in 6 M GdmCl. The assay was carried out in triplicate. The values obtained in individual experiments are reported in the table.

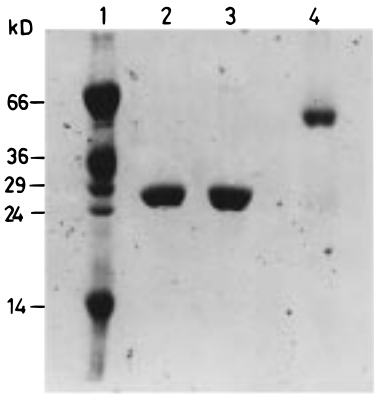

FIGURE 2: SDS−PAGE analysis of purified TIMWT (lane 2) and Y74Cox (lane 4). The wild-type protein migrates at ~27 kDa and Y74Cox is seen to migrate at ~54 kDa. Lane 3 shows the effect of reduction by β-mercaptoethanol on the oxidized mutant. Y74Cred is seen to migrate as a 27 kDa protein upon reduction. Lane 1 shows the molecular mass markers.

Precipitation. The thermal precipitation of the two proteins was followed by monitoring the dependence of Rayleigh scatter intensity on temperature (Figure 5A). The samples were excited at 400 nm, and the scatter was monitored at the same wavelength using a 90° geometry of detection. There is a sharp increase in scatter intensity after 55 °C for both PfTIM and Y74Cox. Both have similar precipitation temperatures (63 and 59 °C, respectively). This heat-induced

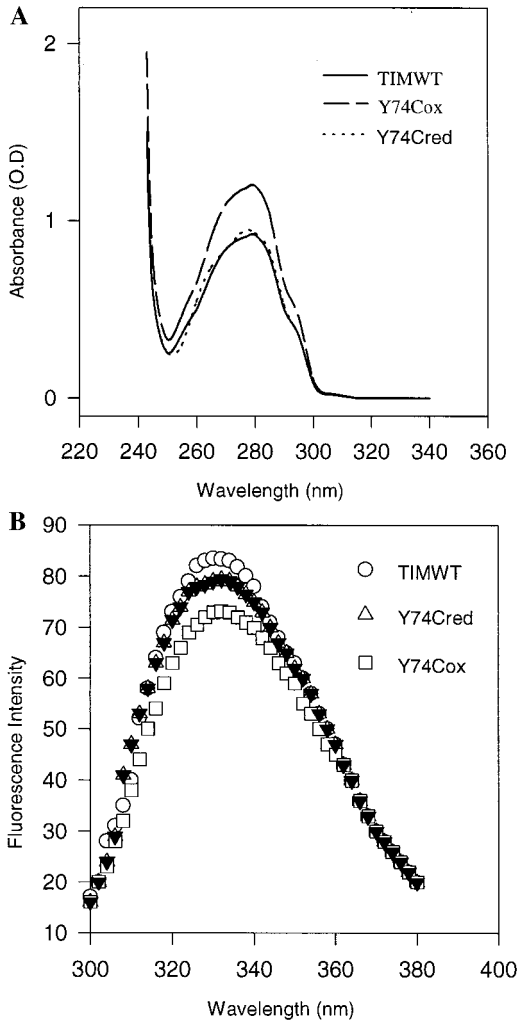

FIGURE 3: (A) Comparison of the UV spectra of TIMWT, Y74Cox, and Y74Cred. All three proteins show absorption maxima at 280 nm. (B) Comparison of the fluorescence emission spectrum of TIMWT, Y74Cox, and Y74Cred following excitation at 280 nm. A protein concentration of 2 μM was used for the measurement. All three proteins show an emission maximum at 331 nm.

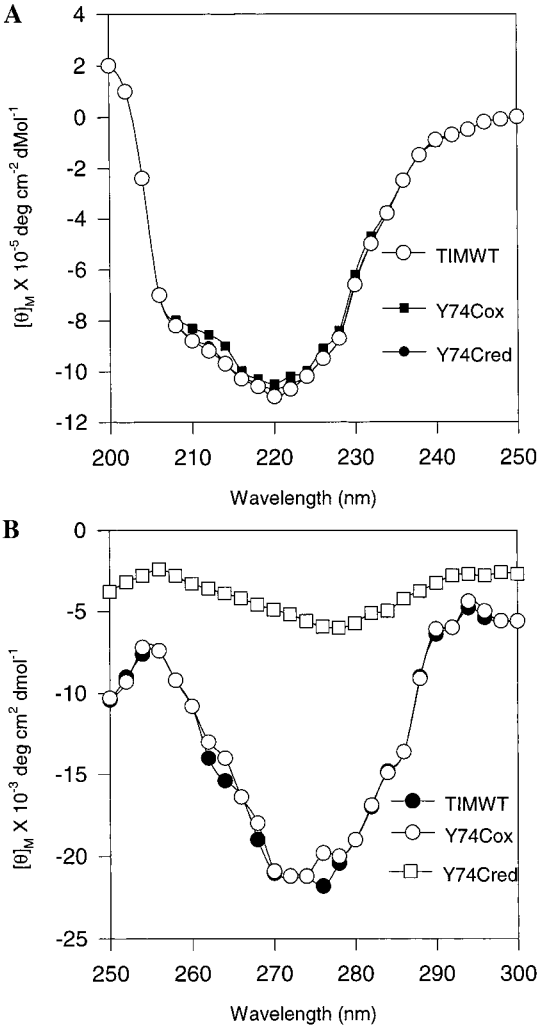

FIGURE 4: (A) Comparison of the far-UV CD spectra of TIMWT, Y74Cox, and Y74Cred. (B) Comparison of near-UV CD spectra of TIMWT, Y74Cox, and Y74Cred.

precipitation was found to be an irreversible process. In sharp contrast, the reduced form of Y74C precipitated at 40 °C indicating that the reduced form was substantially destabilized by the mutation.

Far-UV CD spectra were recorded at various temperatures for TIMWT, Y74Cox, and Y74Cred. TIMWT and Y74Cox show a gradual loss of ellipticity with complete unfolding occurring by 65 °C (Figure 5B). Y74Cred on the other hand shows a sharp transition with complete unfolding occurring by 38 °C. The temperature unfolding data suggest that there are no appreciable differences in the stability of the two proteins PfTIM and Y74Cox, as indicated by the thermal precipitation temperature. Disulfide cross-linking does not seem to have perturbed the overall architecture of the TIM barrel. Further, at 25 °C Y74Cox has 94% of the specific activity of wild-type PfTIM, reinforcing the view that there are no major perturbations in the structure. Interestingly, activity measurements show that the specific activities of PfTIM and Y74Cox differ widely after incubation at an optimum temperature of 40 °C. These results suggest that, although the covalent bridging has not altered the overall stability, it does seem to have modified the flexibility of the PfTIM active site in a subtle way. Since the disulfides are introduced close to the active site, it is likely that covalent tethering has made this region rigid, inhibiting favorable movements of chemical groups needed for catalysis.

Structural Analysis. Data collection and refinement statistics of the Y74C mutant are shown in Table 3. The crystal structure shows that the mutation has not affected the overall structure of PfTIM. An interesting observation made during the course of model building was that only one of the two symmetry-related positions has a density corresponding to a disulfide bridge (Figure 6A). This was verified by a series of omit-map calculations for segments around the mutation site. The corresponding cystines at this position (13−74′) showed the distance between the sulfur atoms to be 2.26 Å, $\chi_{ss} = 120.09°$, stereochemistry suited for the formation of the disulfide bond (Figure 6A). The density around the other site (74−13′), however, clearly did not show the connectivity for the disulfide bridge (Figure 6B). Also no density corresponding to a DTT molecule or water was found close to this site. The distance between the two sulfur atoms in this case was 6.68 Å (Figure 6B), effectively ruling out disulfide bond formation. Figure 7 shows the superposition of TIMwt (light tube) and Y74C (dark tube) at the site of mutation. The conspicuous difference is seen in the case of

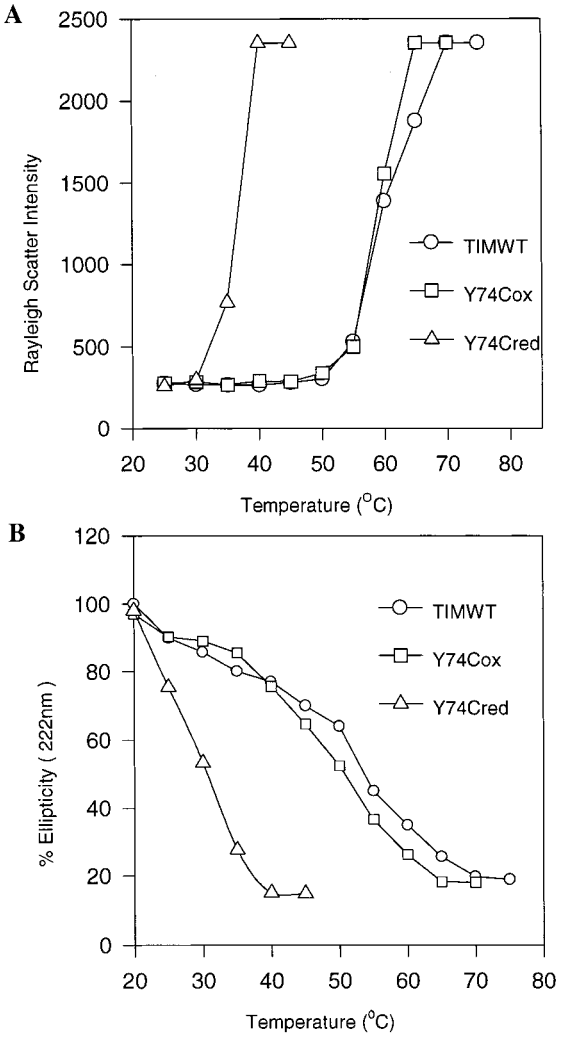

FIGURE 5: (A) Comparison of thermal precipitation of TIMWT, Y74Cox, and Y74Cred monitored by Rayleigh scattering intensity at 400 nm. A protein concentration of 2 μM (100 mM TrisCl, pH 8.0) was used. (B) CD ellipticity of TIMWT, Y74Cox, and Y74Cred at 220 nm (θ_{220}) as a function of temperature. The protein concentration was 8 μM (100 mM TrisCl, pH 8.0), and the path length was 0.1 mm. The ellipticity value at 25 °C was taken as 100%.

Table 3: Summary of Crystallographic Data and Refinement Statistics

total no. of reflections measured	71 498
av. no. of times each intensity was estimated	3.1
total no. of unique reflections	23 064
no. of unique reflections in the resolution range 10−2.2 Å with $I/\sigma(I) > 2.0$	8 760
completeness in the resolution range 10−2.2 Å with $I/\sigma(I) > 2.0$	95.4%
completeness in the last resolution shell 2.34−2.2 Å	77.17%
R-merge[a]	8.81%
initial R^a factor for the PfTIM model in the cell of Y74C	39.7%
initial free R^a factor for the PfTIM model in the cell of Y74C	40.5%
final R^a factor for reflections with $I/\sigma(I) > 2.0$ in the resolution range 10.0−2.4 Å	24.3%
final free R^a factor for reflections with $I/\sigma(I) > 2.0$ in the resolution range 10.0−2.4 Å	27.9%
no. of non-hydrogen atoms in the model	4 075
RMS deviation in bond angles (deg)	1.42
RMS deviation in bond lengths (Å)	0.008

[a] Defined as $\sum |F_o - kF_c|/\sum F_o(100)$.

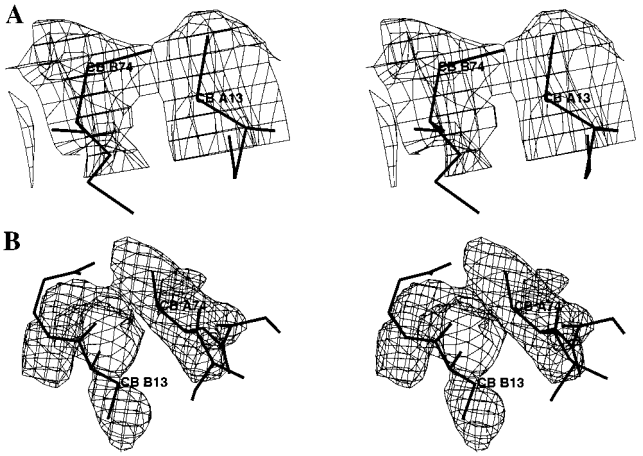

FIGURE 6: (A) $2F_o - F_c$ electron density maps at the oxidized site 13−74′. The disulfide density and approximate orthogonal geometry about the S−S bond are depicted. (B) The reduced site 74−13′. Note the absence of density between the sulfur atoms. The C−S bonds in this case point away from one another.

the oxidized site (Figure 7A) where the main chain caves in to fill the cavity. Figure 8 shows the superposition of TIMwt (light tube) and the Y74C mutant (dark tube) at the active sites. Lys 12, which is adjacent to the site of mutation, is a key residue at the active site and has been shown to adopt an unusual positive phi value in all of the TIM crystal structures solved so far. Replacement of Tyr 74 by Cys and consequent disulfide bond formation to Cys 13 do not significantly affect the positioning of the three active site residues His 95, Phe 96, and Glu 165. The active site geometries are similar within limits imposed by the current resolution (2.4 Å) at both the oxidized and reduced sites. The somewhat lower enzymatic activity observed for the bis-disulfide form may be an indicator of an altered active site geometry. Unfortunately, crystallographic characterization of this form could not be achieved.

DISCUSSION

There is a vast amount of literature on mutations leading to cavities in the protein core. Most studies have focused on small, monomeric, globular proteins for which high-resolution crystal structures have been determined for both the wild-type and mutant structures. Representative examples include T4 lysozyme (*25*), ribonuclease A (*26*), λ repressor (*27*), staphyloccocal nuclease (*28*, *29*), and chymotrypsin inhibitor 2 (*30*). These studies demonstrate that there may be a correlation between the volume of the cavity created in the protein interior and the reduction in the stability (*31*). Furthermore, the kind of amino acid replacement (polar or nonpolar) in the protein interior seems to be important for protein stability (*32*, *33*).

In PfTIM, introduction of a Cys residue in the place of a Tyr at the interface results in pronounced instability of the reduced mutant Y74Cred. Oxidation to the bis-disulfide Y74Cox enhances the stability of the protein with respect to the dithiol form. Disulfide bridging thus appears to compensate for the effects of the cavity-forming mutation at the subunit interface of the dimeric protein. In the earlier example of disulfide engineering across the subunit interface of thymidylate synthase (*11*), it was suggested that covalent cross-linking may be a general means of enhancing the

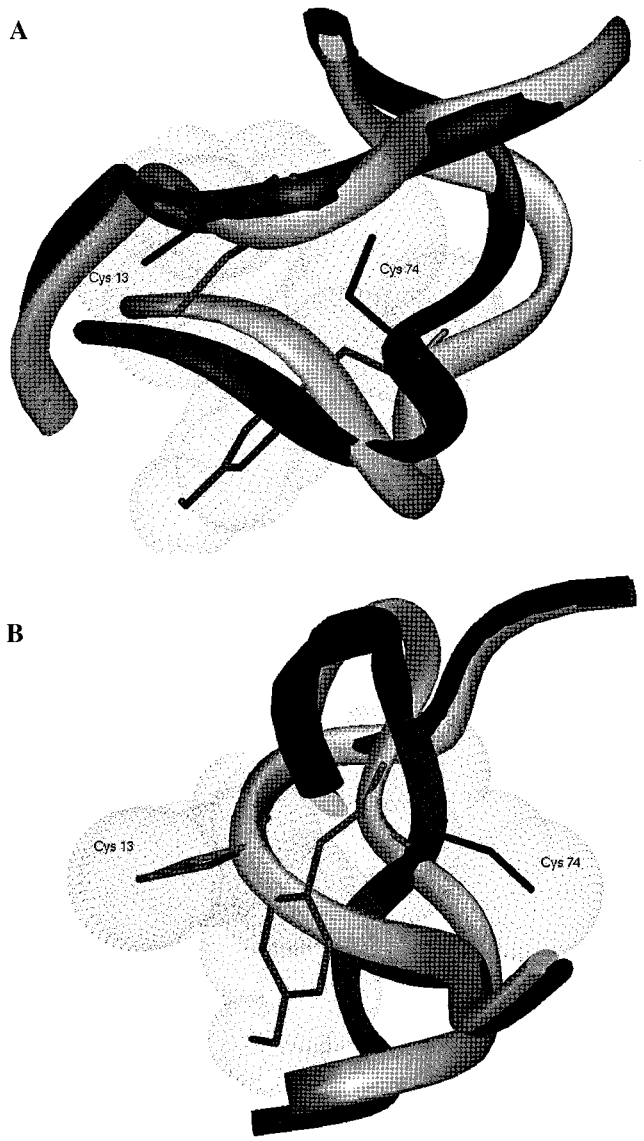

FIGURE 7: Superposition of TIMwt (light tube) and Y74C (dark tube) structures at the site of mutation. Shown in A is the oxidized site and in B is the reduced site. The most conspicuous difference is the movement of the main chain in the reduced form (B) as compared to PfTIM. This could be contrasted to the oxidized counterpart (A), where the main chain caves in to reduce the cavity.

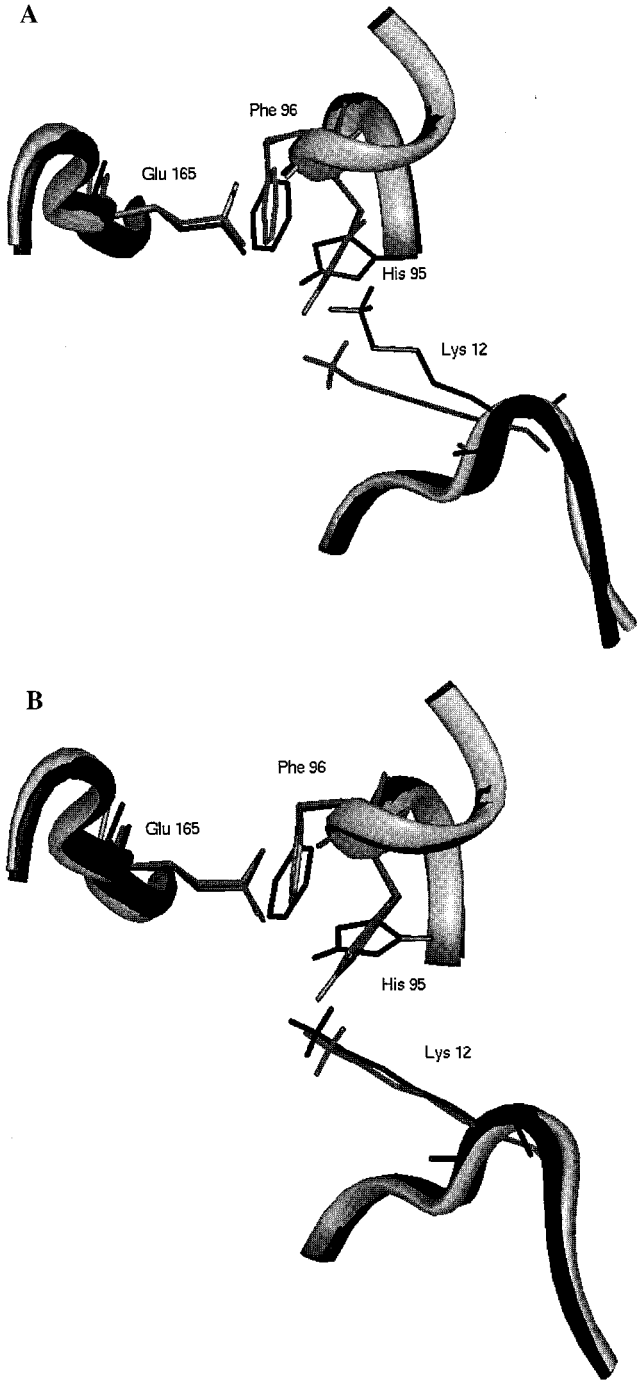

FIGURE 8: Superposition of the active site residues of PfTIM (light tube) and Y74C (dark tube). In A is the oxidized form and in B, the reduced. The side chain rotamer of Lys 12, the active site residue closest to the disulfide bond forming Cys 13, is different from PfTIM.

stability of multimeric enzymes. However, results of disulfide engineering need to be interpreted with caution, since the mutation may itself prove to be destabilizing, as observed for the present case of PfTIM. The failure of repeated attempts to crystallize the bis-disulfide form of the mutant in the absence of trace quantities of reducing agents could imply that this form is inherently less crystallizable. Upon the addition of trace quantities of DTT, one of the disulfide bonds gets reduced. This then yielded crystals suitable for structural studies. The observation of only one disulfide bridge between molecules related by 2-fold noncrystallographic symmetry suggests that the asymmetry that exists in the partially reduced enzyme has influenced crystallization. The structure of the partially reduced mutant thus offers insights into the structures of both the disulfide-bonded as well as the reduced forms of the mutant.

The mutation to a smaller and more polar residue at the interface has probably diminished the favorable intermolecular interactions in the dimeric protein. Figure 7 compares the space-filling model of the native and the mutant proteins at the site of mutation. An examination of the crystal structure of PfTIM suggested that the residue Tyr at position 74 makes crucial contacts with Tyr 101′ and Phe 102′ across the subunit interface. In addition to the breakdown of the interaction between Y74 and F102′, replacement of Tyr with Cys might also lead to a cavity of ~50 Å^3, as calculated from the van der Waals volume of the two residues. The crystal structure of the partially oxidized Y74C mutant provides an opportunity to evaluate the sizes of the cavities created by the

Table 4: Effects of Interface Mutations on TIM Stability

interface mutants	T_m of wild type	T_m of mutant	reference
trypanosomal TIM (deletions in loop 3 [residues 69−74])	44 °C	38 °C	Wierenga et al., 1994
trypanosomal TIM (H47N)	44 °C	33 °C	Wierenga et al., 1993
yeast TIM (N78D)	58 °C	44 °C	Klibanov et al., 1987
human TIM (M14Q)	55 °C	48 °C	Hol et al., 1996
human TIM (R98Q)	55 °C	48 °C	Hol et al., 1996
Plasmodium falciparum TIM (Y74C)	65 °C	59 °C (oxidized), 38 °C (reduced)	this manuscript

mutations at both the oxidized and reduced sites. Cavity calculations performed using the program VOIDOO (*34*) employing a probe radius of 1.4 Å reveal a cavity size of approximately 100 Å^3 at the reduced site while the cavity volume at the oxidized site is about 40 Å^3 thus showing an increase in the cavity size by ∼60 Å^3 around the site of mutation in the reduced form of the protein when compared to its oxidized counterpart. The reduction of the size of the cavity in the oxidized form from the anticipated value appears to be due to the concerted movement of the residues lining the cavity. The effects of cavity-creating mutations in the interior of proteins have been extensively studied in T4 lysozyme (*25*) and ribonuclease A (*26*). Crystal structures show that interior residues are packed together in such a manner as to ensure optimal space filling without large cavities and with no steric overlaps between residues. These observations clearly point to the importance of packing interactions in determining the protein fold (*35*). Interestingly, protein structures have been shown to be remarkably tolerant to single-site substitutions, suggesting structural plasticity, such that mutations at most of the positions in a sequence can be tolerated with no dramatic, deleterious effects on the protein stability (*31*, *33*, *36*). Experimental studies have shown that the introduction of cavities in the interior of proteins is generally partially compensated by rearrangements in the surrounding protein side chains (*33*, *35*). In contrast, the effects of cavity-creating mutations at the interface between subunits in multimeric proteins have not been probed in detail (*33*). As illustrated in this study, replacement of Tyr with Cys in PfTIM has decreased the precipitation temperature by 20 °C. Such large changes in protein stability, introduced by single-site mutation, are not common even when the mutations are in the protein core.

Triosephosphate isomerases from diverse sources appear to be quite sensitive to mutations at the dimer interface. Table 4 summarizes the effect of mutations in the thermal melting temperature (T_m). While all reported mutations appear to lower T_m, the largest change observed so far is for the reduced form of the Y74C mutant of PfTIM. A particularly noteworthy feature of the present study is the dramatic stabilization ($\Delta T_m = 21°$) that occurs upon oxidation to form the bis-disulfide mutant. The Y74C mutation is destabilizing because of the cavity formation and the loss of important intersubunit contacts involving residues Tyr 101 and Phe 102. Covalent cross-linking of the two subunits largely offsets this destabilizing factor. The initial motivation for the studies described in this paper was to use disulfide engineering as a means of stabilizing the dimeric enzyme PfTIM. In attempting to use a pre-existing Cys residue at position 13, the choice of mutation sites was restricted to position 74. However, replacement of a large aromatic residue Tyr by a smaller residue Cys in the hydrophobic region of the interface results in a substantial loss of stability for the non-cross-linked dimer. Sites chosen for disulfide engineering must therefore be carefully evaluated for the possible effects of a mutation. Buttressing protein interfaces with multiple disulfide bridges, avoiding complications that could arise due to large changes in residue volumes upon mutation, appears to be a promising approach for stabilizing multimeric protein structures.

ACKNOWLEDGMENT

We acknowledge the Interactive Computer Graphics Facility supported by the Department of Biotechnology and the National Area Detector Facility.

REFERENCES

1. Tsong, T. Y., Hearn, R. P., Wrathall, D. P., and Sturtevant J. M. (1970) *Biochemistry 9*, 2666−2677.
2. Wells, J. A., and Powers, D. B. (1986) *J. Biol. Chem. 261*, 6564−6570.
3. Ahren, T. J., and Klibanov, A. M. (1985) *Science 238*, 1280−1284.
4. Zale, S. E., and Klibanov, A. M. (1986) *Biochemistry 25*, 5432−5444.
5. Hempstead, P. D., Yewdall, S. J., Fernie, S. J., Lawson, S. J., Artymiuk, S. J., Rice, S. J., Ford, S. J., and Hensel, R. (1993) Proteins of extreme thermophiles, in *The Biochemistry of the Archaea* (Kates, M., Kushner D. J., and Matheson, A. T., Eds.) pp 209−221, Elsevier, Amsterdam, The Netherlands.
6. Russel, R. J. M., and Taylor, G. L. (1995) *Curr. Opin. Struct. Biol. 6*, 370−374.
7. Sauer, R. T., Hehir, K., Stearman, R. S., Weiss, M. A., Jeitler-Nilsson, A., Suchanek, E. G., and Pabo, C. O. (1986) *Biochemistry 25*, 5992−5998.
8. Shirakawa, M. S., Matsuo, H., and Kyogoku, Y. (1991) *Protein Sci. 4*, 545−552.
9. Scrutton, N. S., Berry, A., and Perham, R. N. (1988) *FEBS Lett. 241*, 46−50.
10. Wakarchung, W. W., Sung, W. L., Campbell, R. L., Cunningham, A., Watson, D. C., and Yaguchi, M. (1994) *Protein Eng. 7*, 1379−1386.
11. Gokhale, R. S., Agarwalla, S., Francis, V. S., Santi, D. V., and Balaram, P. (1994) *J. Mol. Biol. 235*, 89−94.
12. Agarwalla, S., Gokhale, R. S., Santi, D. V., and Balaram, P. (1996) *Protein Sci. 5*, 270−277.
13. Gokhale, R. S., Agarwalla, S., Santi, D. V., and Balaram, P. (1996) *Biochemistry 35*, 7150−7158.
14. Tamma, A., and Privalov, P. L. (1998) *J. Mol. Biol. 273*, 1048−1051.
15. Wierenga, R. K., Noble, M. E. M., Vriend, G., Nauche, S., and Hol, W. G. J. (1991) *J. Mol. Biol. 220*, 995−1015.
16. Ranie, J., Kumar, V. P., and Balaram, H. (1993) *Mol. Biochem. Parasitol. 61*, 159−170.
17. Anderson, A., and Cooper, R. A. (1970) *J. Gen. Microbiol. 62*, 324−329.
18. Velanker, S. S., Ray, S. S., Gokhale, R. S., Suma, S., Balaram, H., Balaram, P., and Murthy, M. R. N. (1997) *Structure 5*, 751−761.
19. Kunkel, T. A., Roberts, J. D., and Zakour, R. A. (1987) *Methods Enzymol. 154*, 367.
20. Ellman, G. L. (1959) *Arch. Biochem. Biophys. 82*, 70−77.
21. Navaza, J. (1994) *Acta Crystallogr., Sect. A 50*, 157−163.
22. Brunger, A. T. (1992) X-Plor, Version 3.1 *A system for X-ray Crystallography and NMR*, Yale University Press, New Haven, CT.
23. Sowdhamini, R., Srinivasan, N., Shoichet, B., Santi, D. V., Ramakrishnan, C., and Balaram, P. (1989) *Protein Eng. 3*, 95−103.
24. Holmgren, A. (1981) *Trends Biochem. Sci. 6*, 26−29.

25. Baldwin, E. P., and Matthews, B. W. (1994) *Curr. Opin. Biotechnol. 5*, 396−402.
26. Varadarajan, R., and Richards, F. M. (1992) *Biochemistry 31*, 12315−12327.
27. Milla, M. E., and Sauer, R. T. (1995) *Biochemistry 34*, 3344−3351.
28. Shortle, D., Meeker, A. K., and Freire, E. (1988) *Biochemistry 27*, 4761−4768.
29. Stites, W. E., Gittis, A. G., Lattman, E. E., and Shortle D. (1991) *J. Mol. Biol. 221*, 7−14.
30. Jackson, S. E., Moracci, M., elMasry, N., Johnson, C. M., and Fersht, A. R. (1993) *Biochemistry 32*, 11259−11269.
31. Lim, W. A., and Sauer, R. T. (1991) *J. Mol. Biol. 219*, 359−376.
32. Hubbord, S. J., and Argos, P. (1994) *Protein Sci. 3*, 2194−2206.
33. Hubbord, S. J., and Argos, P. (1995) *Curr. Opin. Biotechnol. 6*, 375−381.
34. Kleywegt, G. J., and Jones, T. A. (1996) *Acta Crystallogr., Sect. D 52*, 826−828.
35. Richards, F. M., and Lim, W. A. (1994) *Annu. Rev. Biophys. 26*, 423−498.
36. Matthews, B. W. (1993) *Annu. Rev. Biochem. 62*, 139−160.

BI981495W